Journal of Power Sources, 46 (1993) 299–310

New aspects of the solid phase equilibria in the ternary Pb–Sn–Ca system for $x_{Ca} \leq 25$ at.%

J. Hertz, C. Fornasieri, J.P. Hilger and M. Notin

Laboratoire de Thermodynamique Métallurgique, URA CNRS 1108, Université de Nancy I, B.P. 239, 54506 Vandoeuvre-Les-Nancy Cedex (France)

Abstract

New crystallographic data prove that $CaPb_3$ and Sn_3Ca–$L1_2$ compounds belong to the same single-phase $Ca(Pb, Sn)_3$ domain in the ternary Pb–Sn–Ca equilibrium phase diagram. A tentative calculation of this diagram shows that about 2 wt.% Sn, introduced in the α-Pb matrix, allows a decrease in the solubility of Ca at 400 K from 10^{-2} to 10^{-7} wt.%. Simultaneously, the $L1_2$ compound, in equilibrium with the α-Pb matrix, crosses very rapidly the $x_{Ca} = 0.25$ line, continuously from the Pb–Ca border to near the Sn–Ca border, when increasing the Sn content in the α matrix from zero to 8 wt.% Sn at 400 K. A very large triangle formed by the three phases α-Pb (8 wt.% Sn), β-Sn (1.7 wt.% Pb), $Ca_{25}Pb_5Sn_{70}$–$L1_2$ appears in this diagram at 400 K. This triangle provides a ternary eutectic, calculated at 424 K. This calculation brings to light some reasons for the process transition for the hardening of Pb–Ca grid-battery alloys, from discontinuous to continuous, when increasing the tin content.

Literature surview of Pb–Ca and Pb–Sn–Ca age hardening

Lead hardening by calcium is a very complicated phenomenon. A very small amount of Ca in a binary Pb–Ca matrix, (e.g., 0.06 wt.% Ca) is sufficient to obtain, after a rapid cooling of the alloy, an oversaturated matrix, suitable for rapid age hardening at room temperature. The hardening process of binary Pb–Ca alloys belongs to the so-called discontinuous reaction. This is linked to the rapid scanning of each grain, over time, by two successive reaction fronts that move with a very low activation energy (of about 11 to 20 kJ/mol [1, 2] for the first stage). By contrast, the hardening process of the ternary Pb–Sn–Ca alloys, with a weight ratio $w_{Sn}/w_{Ca} \geq 9$, belongs to the more classical continuous structural hardening by bulk precipitation of a $L1_2$ phase, finely dispersed in the matrix. Technologically, the discrepancy between the binary Pb–Ca and ternary Pb–Sn–Ca behaviour can be used to choose either a fast hardening process (with low Sn content) or a delayed hardening process (with high Sn level). A two-fold hardening, in two separate stages, can also be obtained by using an intermediate Sn/Ca ratio. This fact is well known in the community of lead and battery producers. But, up to now, the scientific reasons for such a modification of the age hardening, by Sn, has been largely ignored.

Scharfenberger and Henkel [3] have described the hardening process of binary Pb–Ca alloys containing up to 0.08 wt.% Ca in terms of two stages, and have attributed the hardening to an unobserved hypothetical coherent precipitation of a dispersed $CaPb_3$–$L1_2$ phase. Borchers and Assmann [4] have shown that 'the discontinuous precipitated coherent $CaPb_3$ phase of the binary system changes by increasing Sn

0378-7753/93/$6.00

addition into a more Sn-rich $Ca(Pb, Sn)_3$ phase which also precipitates homogeneously'. We have claimed [5] that the high electronic microscopy resolution does not confirm any precipitation in binary Pb–Ca alloys, after the two rapid stages hardening, but only the organization of the whole matrix in small (about 10 nm wide) domains. Very recently, Tsubakino *et al.* [6] published a new transmission electron microscopy (TEM) study of the age-hardening process in the Pb–0.08wt.%Ca alloy. Their observations lead to the same conclusion as our preceding publication [5], that no precipitation occurs during the rapid age hardening of the binary Pb–Ca alloys. From resistivity measurements, the same authors have determined a Tc line in the $\alpha + CaPb_3$ equilibrium domain. Below the Tc line, the discontinuous process is active. We consider this line as a spinodal border line. Above the Tc line, only the continuous precipitation of $CaPb_3$–$L1_2$ is observed.

Hilger *et al.* [7] provided an optical microscopic method to follow the front of the two first discontinuous reactions by using polishing at −50 °C and chemical attack at 20 °C after repeated isochronal hardening at room temperature. By this method, they have measured [1, 2] the mean rate of the moving of these reaction fronts at room temperature: about 3 to 10 μm min^{-1} for the first epitaxic rectilinear front and about 1 μm min^{-1} for the second reaction that provides the puzzle aspect of the grain boundaries. These two reactions do not imply any precipitation. The activation energy of the first hardening process was measured between 20 and 70 °C and the result was of the order of 11 to 20 kJ mol^{-1}; this is very small in comparison with the autodiffusion activation energy for Pb, i.e., about 104 kJ mol^{-1}.

Adeva *et al.* [8] have investigated, by X-ray diffraction (XRD), the Pb-rich corner of the Pb–Sn–Ca phase diagram up to 0.2 wt.% Ca and 3.0 wt.% Sn. Their method consisted of measuring the lattice parameter of the α-Pb-face-centred cubic (f.c.c.) matrix. The quantity of any other phase in equilibrium was too small to be analysed by XRD. The conclusion of this work (Fig. 1) was that three phases can be present, simultaneously, to provide a constant lattice parameter of the α matrix. The other two are not clearly identified, but the authors suggested, without any real proof, that these two phases could be $CaPb_3$ and $CaSn_3$ and were present simultaneously. Prengaman [9] also described the Pb-rich corner of the ternary Pb–Sn–Ca phase

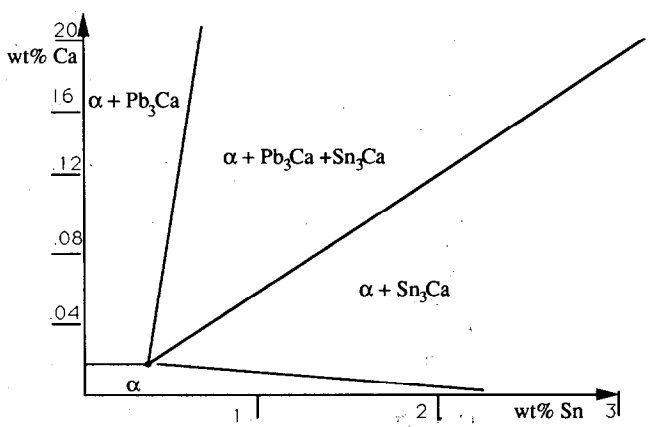

Fig. 1. Isothermal cut of the Pb–Sn–Ca phase diagram at room temperature in the area surrounding the α-Pb matrix, taken from Adeva *et al.* [8].

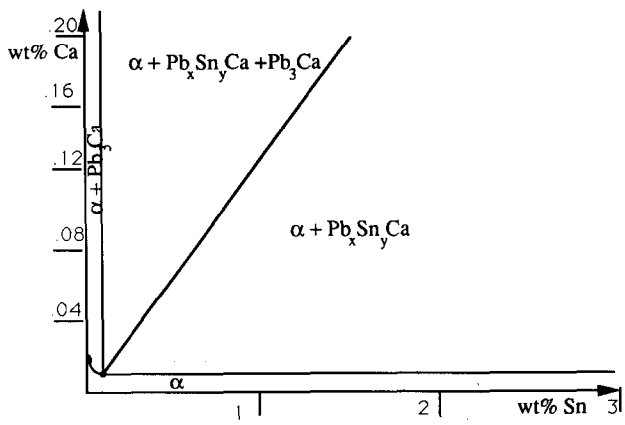

Fig. 2. A schematic isothermal cut, at room temperature, of the Pb–Sn–Ca phase diagram near the α-Pb matrix, according to the predictions of Prengaman [9].

diagram (Fig. 2) as a three-phase domain, connected with the $\alpha+CaPb_3$ border. In this opinion, the new phase in the triangle could be $Ca(Pb, Sn)_3$.

Crystallographic and differential thermal analysis studies

In our opinion, $CaPb_3$ and $CaSn_3$ belong to the same single-phase domain in the equilibrium phase-diagram and, for this reason, we decided to reinvestigate the crystallography of the $x_{Ca}=0.25$ at.% line in the ternary diagram. The aim of this work was to establish whether there is only one $L1_2$ phase, starting from $CaPb_3$ up to $CaSn_3$, that follows every $Ca(Pb, Sn)_3$ composition.

Eleven $Ca(Pb, Sn)_3$ mixtures were elaborated in an iron crucible and sealed under argon in a glove-box. The following Sn/Pb mole ratios were chosen: 0/10, 1/9, 2/8, 3/7, 4/6, 5/5, 6/4, 7/3, 8/2, 9/1, 10/0. The alloys were melted at 876 °C under purified argon. After low-rate cooling, each sample was separated into three parts.

The first part was powdered under purified argon and sealed in a glass capillary tube for XRD analysis. These precautions are needed because of the high reactivity of the $L1_2$ phase with air, when powdered [10]. Diamond powder was mixed in the capillary tube to calibrate the X-ray lattice parameters. The second part of the sample was analysed between 20 and 900 °C under argon in a differential thermal analyser (DTA method.) The third part was devoted to microprobe analysis.

The results obtained with the three methods are consistent with the sole conclusion that $CaPb_3$ and $CaSn_3$ form a continuous line of homogeneous solution in the ternary phase diagram from one binary border up to the second one. The following observations were made.

(i) Microprobe analyses of the samples are only semiquantitative because of the rapid decomposition of the $L1_2$ compound during polishing of the samples. Nevertheless, Table 1 indicates that the Ca mole fraction is not too far from 25 mol% and that the x_{Sn}/x_{Pb} ratio varies continuously.

(ii) In spite of the fact that all the DTA curves were not completely successful, because of the high reactivity of the $L1_2$ phase with traces of oxygen, the measured liquidus points seem to follow a continuous curve with a minimum in the middle

TABLE 1

Semiquantitative electron microprobe analysis of samples (mean values)

x_{Sn}/x_{Pb} goal	0	0.11	0.25	0.43	1	1.5	2.33	9	∞
x_{Sn}/x_{Pb} measured	0	0.25	0.30	0.53	2.5	2	1.18	14	∞
x_{Ca} measured (goal = 0.25)	0.23	0.24	0.21	0.21	0.32	0.20	0.07	0.17	0.10

TABLE 2

Semiquantitative liquidus line of $L1_2$ $Ca(Pb, Sn)_3$ phase versus composition obtained by DTA and eutectic points

x_{Sn}/x_{Pb}	0/10	1/9	2/8	3/7	6/4	7/3	8/2	9/1	∞
x_{Xn}	0	0.075	0.15	0.225	0.45	0.525	0.60	0.675	0.75
x_{Pb}	0.75	0.675	0.60	0.525	0.30	0.225	0.15	0.075	0
Liquidus θ °C	647	625	625	614	607			615	627
Eutectic θ °C	328	308	315	304	177	176 ternary eutectic	176	177	220

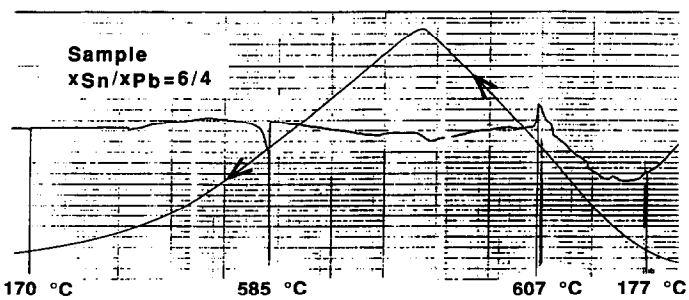

Fig. 3. Second heating/cooling DTA/x curve with $x_{Sn}/x_{Pb}=6/4$, $L1_2$ sample. The liquidus line is observed at 607 °C. Due to loss of calcium, a small eutectic peak is observed at 177 °C on heating. This corresponds to the ternary eutectic invariant. The peak is absent on the first heating curve.

region of the $x_{Ca}=0.25$ plane, see Table 2. Some eutectic points were also detected (Figs. 3 and 4) in the first or second heating (after a Ca loss).

The values proposed in Table 2 cannot be considered as quantitative determinations of the liquidus temperatures, but indicate the direction of the slope. Only the first and last values have been well established by Bouirden [10].

(iii) The more significant proof of the continuity of the $Ca(Pb, Sn)_3$ phase was provided by the XRD analysis of its cubic-lattice parameter. Table 3 gives the measured values: a loss of Ca is always observed during the synthesis process. For this reason, one or two other phases are simultaneously present in the XRD pattern, together with the main $L1_2$ phase. Table 3 shows the subsidiary phases that were observed with each sample. It appears that only pure Pb* with a constant parameter of 0.4955 ± 0.005 nm is detected for $x_{Sn}/x_{Pb} \leq 8/2$. This fact is consistent with the isothermal cut of the phase diagram at low temperature (see, for example, the 400 K cut on

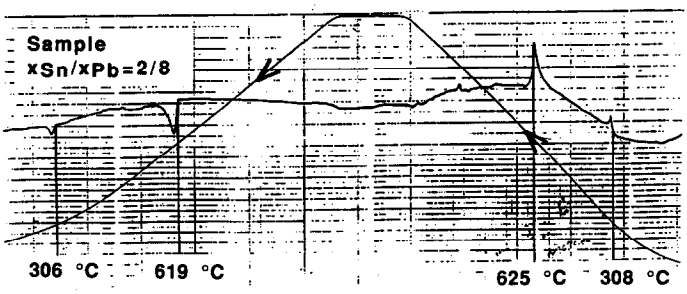

Fig. 4. First heating/cooling DTA/x curve with $x_{Sn}/x_{Pb}=2/8$, $L1_2$ sample. The liquidus line is observed at 625 °C. The eutectic valley ($L1_2$+Pb+liquid) is also detected at 308 °C on heating, linked to a loss of Ca.

TABLE 3

Lattice parameter of the $Ca(Pb, Sn)_3$–$L1_2$ phase vs. composition

x_{Sn}/x_{Pb}	0/10	1/9	2/8	3/7	4/6	5/5	6/4	7/3	8/2	9/1	10/0
x_{Pb}	0.75	0.675	0.60	0.525	0.45	0.375	0.30	0.225	0.15	0.075	0
x_{Sn}	0	0.075	0.15	0.225	0.30	0.375	0.45	0.525	0.60	0.675	0.75
a(nm) ±0.001	0.4916	0.4890	0.4880	0.4844	0.4826	0.4804	0.4803	0.4789	0.4765	0.4763	0.4745
Subsidiary phases	Pb*	Pb*	Pb*	Pb*	Pb*	Pb*	Pb*	Pb*	Pb* +Sn*?	Pb* +Sn*	Sn*

*Pure component.

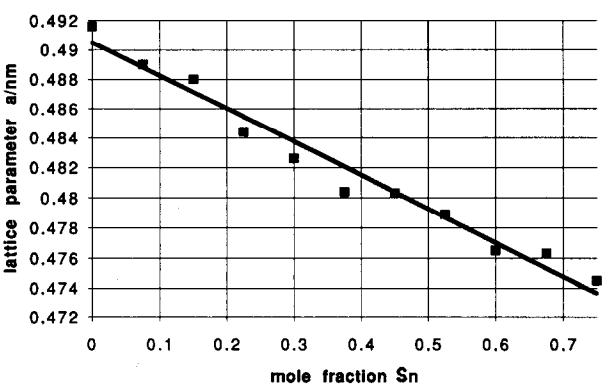

Fig. 5. Variation of cubic lattice parameter of $Ca(Pb, Sn)_3$–$L1_2$ phase vs. Sn content. Experimental uncertainty is of the order of ±0.001 nm.

Fig. 9). Only when $x_{Sn}/x_{Pb}=9/1$ and $=\infty$, is pure Sn* present on the X-ray pattern. Perhaps, some traces are also present for $x_{Sn}/x_{Pb}=8/2$.

Figure 5 shows that the variation of the lattice parameter in the $L1_2$ phase can be fitted by a rectilinear curve versus x_{Sn} or x_{Pb} with the following equations:

$a=(0.4736+0.0225x_{Pb})\pm0.001$ nm

$a=(0.4905-0.0225x_{Sn})\pm0.001$ nm

Recently, Tsubakino *et al.* [11] observed, by TEM, the precipitates in a ternary alloy Pb–0.04wt.%Ca–1.2wt.%Sn. By microdiffraction, they measured a lattice parameter of 0.485 ± 0.02 nm for the precipitates. According to our XRD measurements, the Sn content of such precipitates cannot be readily evaluated with such uncertainty. Nevertheless, by TEM–EDS (energy dispersion spectroscopy) the above authors proved that precipitates were ternary ones.

Tentative thermodynamic calculation of the ternary Pb–Sn–Ca phase diagram for $x_{Ca} \leq 0.25$

Using the Thermo-calc poly-3 program [12], we optimized a phase diagram in the ternary Pb–Sn–Ca system for $x_{Ca} \leq 0.25$. The Pb–Sn binary system was well assessed in the Thermo-calc data bank. For the binary Pb–Ca system, we used our previous assessment and calculation of the Pb–Ca system [13]. The mixing enthalpies of liquid Pb–Ca and Sn–Ca phases have been measured by Bouirden [10], who also determined the enthalpies of formation and the enthalpies and temperatures of melting of the $CaPb_3$ and $CaSn_3$–$L1_2$ compounds. The excess Gibbs energy of the liquid Pb–Ca and Sn–Ca phases was provided by Delcet *et al.* [14]. Nouri *et al.* [15] also measured the excess Gibbs energy for the same binaries, and obtained a good consistency with the previous work by Delcet *et al.* [14]. The solubility of Ca in the α-f.c.c. Pb–Ca matrix was taken in the compilation of Hansen and Anderko [16]. Unfortunately, there is no thermodynamic knowledge of the mixing functions between $CaPb_3$ and $CaSn_3$ in the $Ca(Pb, Sn)_3$–$L1_2$ solution. Thus, an ideal model was adopted.

A Redlich–Kister–Muggianu estimation of the Gibbs energy for the ternary liquid phase was used. Such a calculation allows a semiquantitative ternary equilibrium diagram to be obtained.

Discussion of calculated phase diagram

At first, it must be emphasized that the results are still only qualitative. The ideal assumption used for the $L1_2$ mixing functions provides important quantitative discrepancies with the DTA experiments described here. For example, Fig. 6 compares the calculated liquidus line of the $L1_2$ phase with the measured values (Table 2). It appears that the calculated liquidus surface exhibits an excessively deep basin in the $x_{Ca} = 0.25$ cut, by comparison with DTA.

The three eutectic valleys – (liquid + $L1_2$ + α-Pb) (liquid + $L1_2$ + β-Sn) (liquid + α-Pb + β-Sn) – are convergent in a ternary eutectic equilibrium calculated at 424 K (151 °C) and observed at 176 °C (Table 2). Figure 7 gives the calculated projection of the three valleys, together with the eutectic ternary triangle. The isothermal cut of the ternary phase diagram at 400 K (Fig. 8) shows that the α-Pb matrix draws a curved boundary with the $\alpha + L1_2$ domain, and that about 2 wt.% Sn in the α matrix is sufficient to decrease the solubility of Ca from 10^{-2} to 10^{-7} wt.%. Simultaneously, when increasing the Sn content, the $\alpha + L1_2$ tie line crosses very rapidly the $L1_2$ solid line from the $CaPb_3$ border to near the $CaSn_3$ border (Fig. 9). Figure 10 shows the calculated Pb ratio in the Pb–Sn sublattice of the $Ca(Pb, Sn)_3$–$L1_2$ compound as calculated for $x_{Ca} = 0.06$ wt.%, versus the Sn content of the alloy. A very large three-phase triangle is present in this isothermal cut (400 K, Fig. 9) and has the following

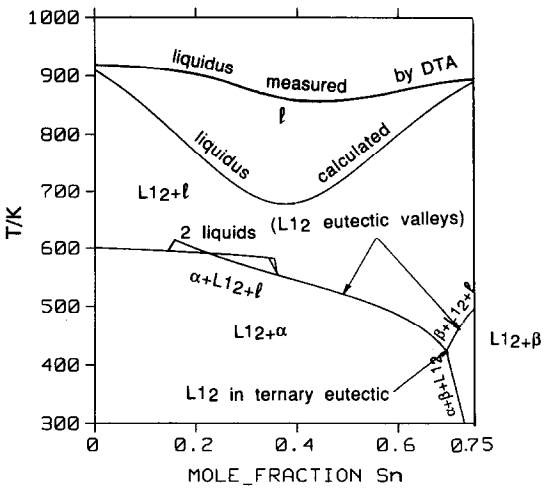

Fig. 6. Calculated $x_{Ca} = 0.25$ isoplethic cut of the Pb–Sn–Ca phase diagram on the border of the α-Pb/$L1_2$ and β-Sn/$L1_2$ equilibria. Calculated lines are the extremities of the tie lines joining the $L1_2$ phase (in the plane of the cut) with the monovariant lines (out of the plane). The calculated liquidus exhibits a basin that is too deep in comparison with the experimental one.

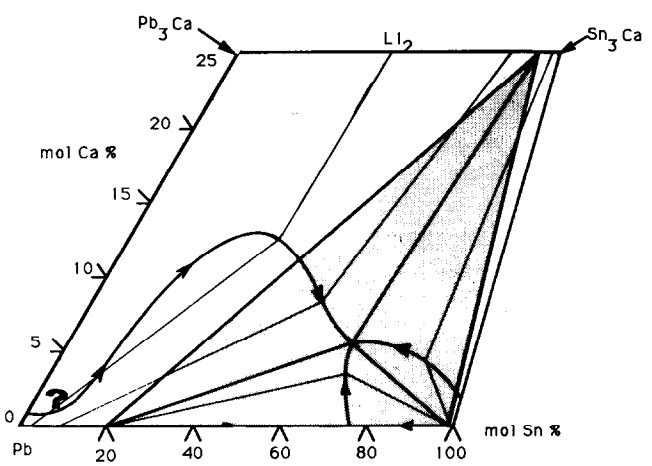

Fig. 7. Projection of the eutectic valleys abstracted from a Thermo-calc calculation, overcharged by many metastable lines. Note the ternary eutectic invariant.

corner phases: α-f.c.c.Pb with 8 wt.% Sn solubility; β-b.c.t.Sn with 1.7 wt.% Pb solubility; $Ca_{25}Pb_5Sn_{70}$–$L1_2$ solid solution (mol%). This triangle is not the three-phase domain detected by Adeva *et al.* [8] at low temperature. Indeed, the present results differ from those of Adeva by the fact that increasing the Sn content in the triangle domain does not cross a biphase boundary at low temperature, but only near the Sn–Ca border. Increasing the temperature in the triangle domain provides the eutectic invariant calculated at 424 K (or 151 °C) and measured at 176 °C (Figs. 6 and 7 and

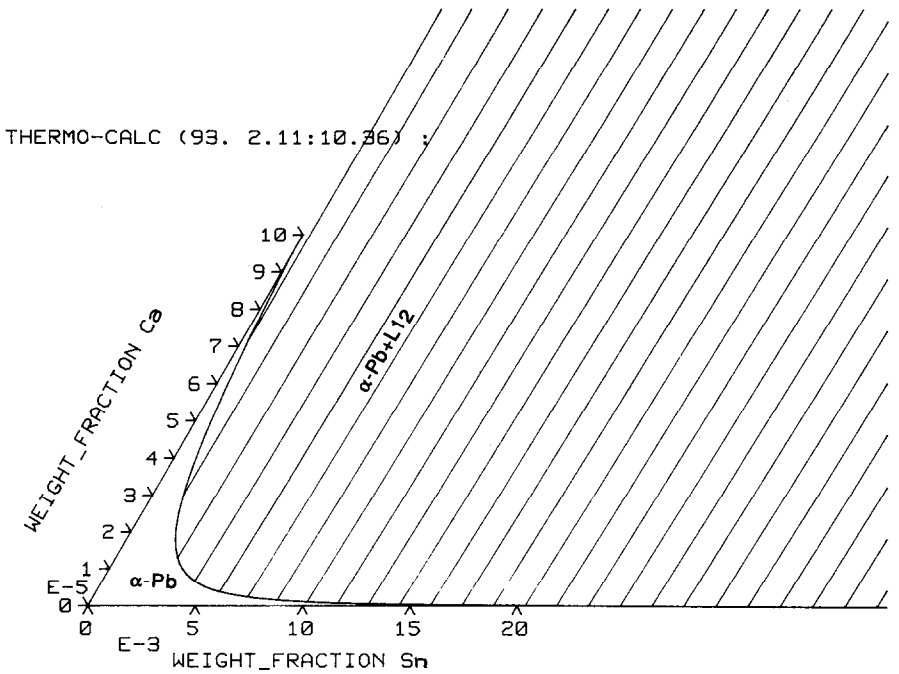

Fig. 8. 127 °C/400 K isothermal cut of Pb–Sn–Ca phase diagram, near the pure-lead corner. Solvus line of α-Pb matrix in equilibrium with $Ca(Pb, Sn)_3$–$L1_2$ phase. Solubility of Ca in the α matrix decreases strongly from 10^{-2} to 10^{-7} wt.% when adding 2 wt.% Sn.

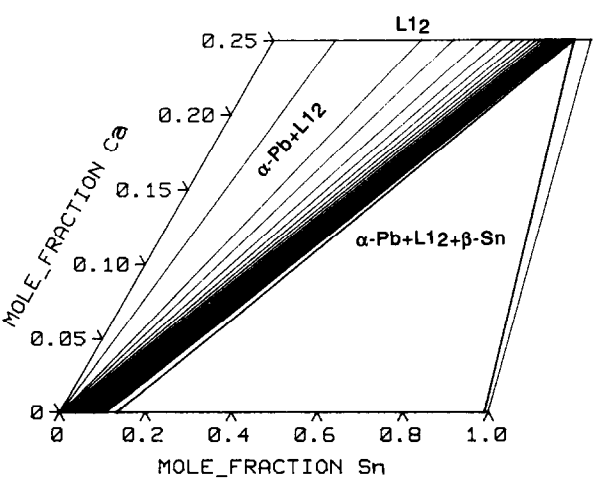

Fig. 9. 127 °C/400 K isothermal cut of Pb–Sn–Ca phase diagram for $x_{Ca} \leq 0.25$. Note the α-$L1_2$ tie lines crossing the $L1_2$ plane from $Ca_{25}Pb_{75}$ to $Ca_{25}Pb_5Sn_{70}$ (in mol%). A large three-phase triangle exhibits an equilibrium between Pb (16 mol% Sn), Sn (3.4 mol% Pb) and $Ca_{25}Pb_5Sn_{70}$–$L1_2$ phase (at 400 K).

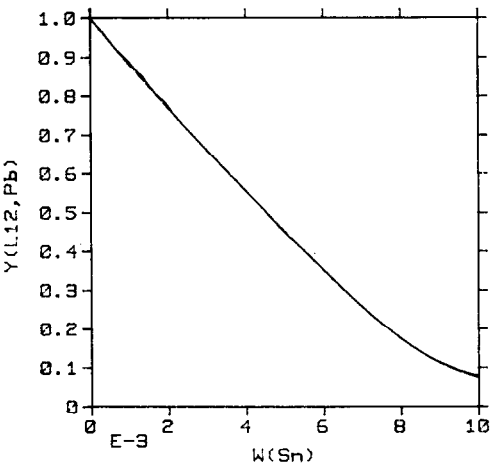

Fig. 10. Calculated $Y = x_{Pb}/(x_{Pb}+x_{Sn})$ ratio vs. Sn mass fraction at 127 °C/400 K in the (Pb, Sn) sublattice of the $L1_2$ phase. The mass fraction of Ca is maintained constant and equal to $w_{Ca}\% = 0.06$. For w_{Sn} increasing from 0 to 1%, the $L1_2$ phase composition varies from $Ca_{25}Pb_{75}$ to $Ca_{25}Pb_5Sn_{70}$.

Table 2). Figure 11 shows the isothermal cut of the diagram at 575 K (or 302 °C). Above 176 °C, the three-phase triangle observed by Adeva *et al.* could be the $L1_2$ + α-Pb + liquid equilibrium.

Discussion of hardening process

According to our calculation the equilibrium solubility of Ca in the α-Pb matrix strongly decreases when increasing the Sn content and when decreasing the temperature. Figures 8 and 12 give the α matrix solvus line calculated at 127 °C (400 K) and 302 °C (575 K). The solubility of Ca is ten times less at 127 °C than at 302 °C, and provides the oversaturated matrix during the quenching process. The 300 °C temperature is often used as rehomogenization treatment before quenching the α phase. It can be observed in Fig. 12 that the two alloys B: Pb–0.6wt.%Sn–0.11wt.%Ca and C: Pb–0.6wt.%Sn–0.06wt.%Ca are on the same $\alpha + L1_2$ tie line and provide the same (M) α matrix during rehomogenization at 300 °C. For this reason, these two alloys have to exhibit about the same hardening process during the ageing period after rehomogenization at 300 °C. This is quite true, according to the results of Bouirden [10], as shown in Fig. 13.

For rehomogenized alloys, the Sn/Ca significant ratio is the ratio of the solvus line and not the absolute ratio of the composition. According to many of Bouirden's [10] results for the rehomogenized alloys, the threshold composition between discontinuous and continuous hardening process can be fixed on the solvus line at about 0.5 wt.% Sn and 0.037 wt.% Ca, point Γ in Fig. 11. In the industrial alloys, the Ca and Sn contents are generally higher than the maximum solubility in the α matrix at 300 °C. With the as-cast products, a part of discontinuous process is always observed. This disappears in the rehomogenized alloys (see Fig. 13).

A spinodal-like rapid hardening by the discontinuous reaction is observed with the Ca-rich α matrix. This corresponds to the upper part of the solvus line (above point Γ, Fig. 11). By contrast, when increasing the Sn content above 0.4 wt.%, the

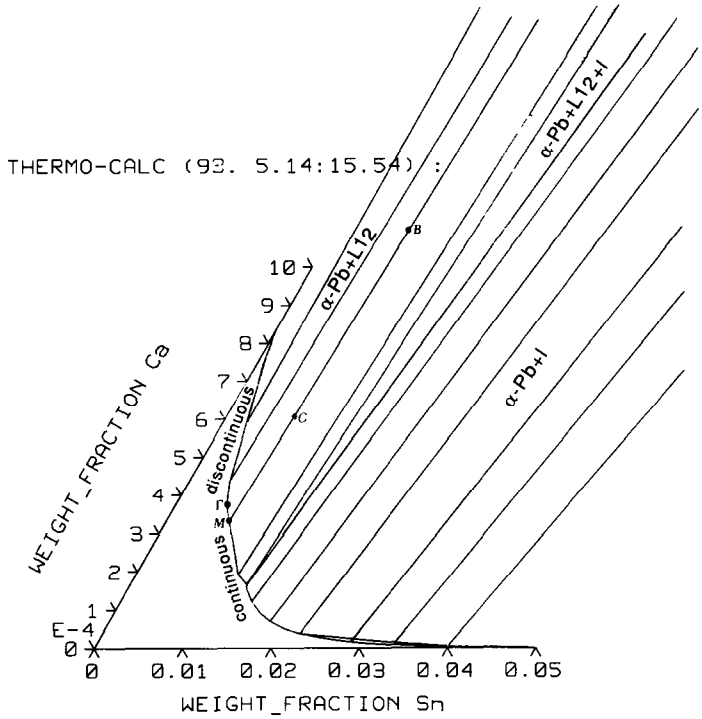

Fig. 11. Calculated 302 °C/575 K isothermal cut of the Pb–Sn–Ca phase diagram, near the pure Pb corner. Note the solvus line of the α-Pb matrix in equilibrium with $L1_2$ phase. Alloys B: Pb–0.6wt.%Sn–0.11wt.%Ca and C: Pb–0.6wt.%Sn–0.06wt.%Ca are on the same tie line corresponding to the same (M) α matrix. After rehomogenization (near 300 °C), these two alloys have the same oversaturated matrix and present quite similar hardening processes at room temperature (see B and C curve in Fig. 13). The threshold between discontinuous and continuous hardening of the α matrix can be fixed on the solvus line at the Γ point.

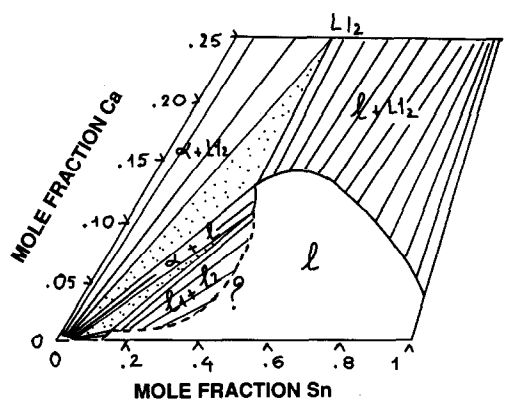

Fig. 12. 302 °C/575 K isothermal cut of the Pb–Sn–Ca phase diagram for $x_{Ca} \leq 0.25$ mol%, abstracted from an overcharged Thermo-calc diagram.

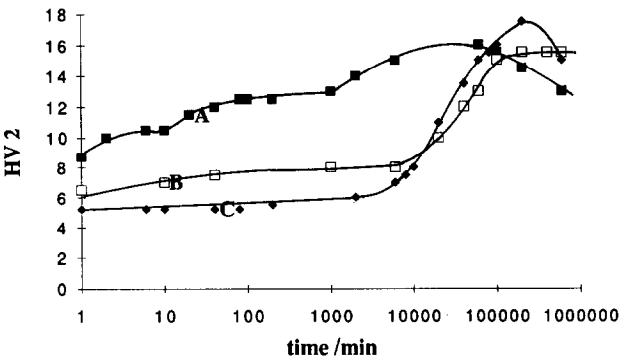

Fig. 13. Hardening curves, at room temperature, of B and C alloys described in Fig. 11. After rehomogenization treatment at 300 °C, these two alloys have the same α-Pb matrix. The two hardening curves look very similar: continuous hardening after an incubation period of 7 days. The richest Ca alloy (B) also shows a slight tendency for rapid discontinuous hardening. This tendency is greatly increased with the as-cast structure (curve A). Composition A: Pb–0.6wt.%Sn–0.06wt.%Ca, and B: Pb–0.6wt.%Sn–0.11wt.%Ca.

continuous bulk precipitation of the $Ca_{25}Pb_5Sn_{70}$-$L1_2$ compound is observed. This is linked to the fact that the α matrix cannot dissolve the Ca. In any case, the $L1_2$ precipitation hardening is much more efficient than the β-Sn precipitation in binary Pb–Sn alloys, by the fact that the $L1_2$ phase remains coherent with the α matrix ($a_{Pb} = 0.495$ nm, $a_{CaPb_3} = 0.490$ nm, $a_{Ca_{25}Pb_5Sn_{70}} = 0.475$ nm).

Acknowledgements

The authors are grateful to Mrs Michèle Lelaurain for obtaining the $L1_2$ XRD patterns, under argon, using her own technique developed at the Laboratory of Mineral Chemistry in Nancy. Thanks are also due to B. Sundman, the Royal Institute of Technology, Stockholm, for the Thermo-calc optimization of the ternary Pb–Sn–Ca thermodynamic functions.

References

1 L. Bouirden, *Thesis*, University of Nancy I, France, Sept. 26, 1990.
2 L. Bouirden, J.P. Hilger and J. Hertz, *J. Power Sources, 33* (1991) 27–50.
3 W. Scharfenberger and S. Henkel, *Z. Metallkd., 64* (1973) 478–483.
4 H. Borchers and H. Assmann, *Z. Metallkd., 69* (1978) 43–49.
5 J.L. Caillerie, J. Hertz, A. Boulharouf, M. Dirand and J.P. Hilger, *Proc. 9th Int. Lead Conf. Goslar, Germany, Oct. 1986,* Lead Development Association, London, UK, 1988, pp. 57–67.
6 H. Tsubakino, R. Nozato and A. Yamamoto, *Z. Metallkd., 84* (1993) 29–32.
7 J.P. Hilger and A. Boulharouf, *Mater. Characteriz., 24* (1990) 159–67.
8 P. Adeva, G. Caruana, M. Aballe and M. Torralba, *Mater. Sci. Eng., 54* (1982) 229–236.
9 R.D. Prengaman, *Electrochemical Society, Fall Meeting, Las Vegas, NV, 1976.*
10 L. Bouirden, *Thesis (3rd cycle)*, University of Nancy I, France, July 11, 1984.
11 H. Tsubakino, R. Nozato and A. Yamamoto, *Scr. Metall. Mater., 26* (1992) 1681–85.

12 B. Sundman, B. Jansson and J.O. Andersson, *Proc. ASM Meet., Orlando, PL, USA, 1986,* reprinted in Thermo-calc documentation set, Division of Physic Metallurgy, Royal Institute of Technology, Stockholm, Sweden.
13 M. Notin, L. Bouirden, E. Belbacha and J. Hertz, *J. Less Common Met., 154* (1989) 121–135.
14 J. Delcet, A. Delgado-Brune and J.J. Egan, in Y.A. Chang and J.F. Smith (eds.), *Calculation of Phase Diagrams and Thermochemistry of Alloy Phases,* Metal. Soc. AIME, New York, 1979.
15 M. Nouri, A. Morisson, M.C. Baron and C. Petot, *Thermochim. Acta, 90* (1985) 207.
16 M. Hansen and K. Anderko, *Constitution of Binary Alloys,* McGraw-Hill, 1958, New York.